

Automatic Quantification of Plant Disease from Field Image Data Using Deep Learning

Kanish Garg, Swati Bhugra, Brejesh Lall
Department of Electrical Engineering
Indian Institute of Technology Delhi

{ee1160446, eez138301, brejesh}@ee.iitd.ac.in

Abstract

Plant disease is a major factor in yield reduction. Thus, plant breeders currently rely on selecting disease-resistant plant cultivars, which involves disease severity rating of a large variety of cultivars. Traditional visual screening of these cultivars is an error-prone process, which necessitates the development of an automatic framework for disease quantification based on field-acquired images using unmanned aerial vehicles (UAVs) to augment the throughput. Since these images are impaired by complex backgrounds, uneven lighting, and densely overlapping leaves, state-of-the-art frameworks formulate the processing pipeline as a dichotomy problem (i.e. presence/absence of disease). However, additional information regarding accurate disease localization and quantification is crucial for breeders. This paper proposes a deep framework for simultaneous segmentation of individual leaf instances and corresponding diseased region using a unified feature map with a multi-task loss function for an end-to-end training. We test the framework on field maize dataset with Northern Leaf Blight (NLB) disease and the experimental results show a disease severity correlation of 73% with the manual ground truth data and run-time efficiency of 5fps.

1. Introduction

Recent awareness to meet the projected food production demands has underlined the importance of effective plant breeding strategies [13]. Despite the improvement in molecular breeding strategies, the plant yield is currently limited by the biotic stress factor i.e. diseases [32]. Therefore, to reduce yield loss, the current breeding strategy is based on the selection of disease-resistant plant cultivars from a large population of cultivars [12]. Traditional visual scoring of the diseased region by domain experts is time-consuming and error prone due to inter/intra rater variability [5]. To augment this screening strategy, various image

based sensors such as visible light imaging, thermal and hyperspectral imaging have been utilised [31]. This, in conjunction with computer vision based methods (also termed as plant disease phenotyping) permits an automatic, accurate and high-throughput disease quantification. In recent years, many methods for plant disease phenotyping have been developed based on visible spectrum (RGB) imaging in contrast to other imaging modalities such as (hyperspectral, thermal etc.), since they require an expensive and sophisticated computational pipeline [19].

Notably, current disease phenotyping methods based on RGB images can be classified into two different problem formulations [31]: (i) Disease detection: defined as an absence or presence of disease region in an image and (ii) Disease quantification: defined as the extent to which individual leaf has been affected. Various computer vision techniques have been used to detect a wide variety of plant diseases [31]. For example, authors in [40] adopted the Hough transform and random forest algorithm to detect early powdery mildew disease. Similarly, machine vision system based on Support vector machine with a radial basis function [7], artificial neural networks [17] and Gaussian mixture models [8] have been developed to detect angular blight, orchid disease and wheat streak mosaic virus respectively. With the advancement of deep learning in computer vision tasks, many recent studies [11, 33] also utilised convolutional neural networks (CNNs) for plant disease detection. Amara et al. [2] used the LeNet model to detect banana leaf diseases whereas Mohanty et al. [25] utilised the GoogleNet model to detect various biotic stress diseases. The previously discussed methods classifies an image in terms of presence or absence of a disease. However, additional information regarding the disease's location and severity plays a pivotal role in current breeding strategies. Thus, the main focus of the paper is disease quantification.

Prior work on disease quantification utilise leaf-level images to extract disease segments. For example, authors in [1, 38] perform Otsu's segmentation algorithm to extract the diseased region from single leaf images. Simi-

larly, Phadikar et al. [27] employed Otsu’s segmentation algorithm in excess green and excess red images [14] for diseased region segmentation. Deep learning based models have also been utilised for this purpose, [19] employed U-net to segment the powdery mildew regions whereas, [36] adopted VGG-16 model to classify the severity of the disease into four stages. The aforementioned methods address a less challenging problem, based on destructive sampling of plant leaves and standardized image acquisition conditions [5]. This results in images with single leaves and uniform background. However, the controlled experiments for disease region segmentation are low-throughput and restricts the temporal study of disease progression. Thus, for precise breeding strategies, a processing pipeline based on field images is desirable. In this respect, unmanned aerial vehicles (UAVs) are used to capture the field images at low altitudes in a high throughput manner.

Field images captured with UAVs suffer from complex backgrounds with densely overlapped leaves, high variability in lighting and perspective conditions. With the advancement of deep learning, especially convolutional neural networks (CNNs), higher recognition accuracy in object detection and segmentation have been achieved [18,42]. Therefore, to tackle the aforementioned irregularities in field images, we present a deep learning framework (shown in Figure 2) that extracts phenotypic traits (such as area, length, etc. of the diseased region) for precise detection and quantification of disease based on field images of maize [39] with Northern Leaf Blight (NLB) disease. However, the dataset presented in [9] does not contain the disease region and leaf instance masks; thus, these labels were generated under the supervision of the experts (details presented in the following section). The proposed framework simultaneously generates segmentation masks for each leaf instance and its corresponding diseased region with a unified feature map and a multi-task loss function for an end-to-end training. The source code is available as a GitHub repository at <https://github.com/kanishgarg/Cascade-MRCNN>. Within the limited literature on this dataset, authors in [9] presented a pipeline based on CNNs for automatic identification of Northern leaf blight (NLB). Notably, this method formulates the disease phenotyping pipelines as a dichotomy case, yielding the presence or absence of disease based on field images. In contrast, another study [35] on NLB dataset utilises Mask-RCNN to only segment the disease region, while the proposed framework also extracts leaf level details in addition to disease segments to capture the extent to which each leaf has been infected, necessary for quantitative evaluation.

In summary, this paper has the following contributions:

- The generation of disease region and leaf instance masks in the existing dataset [39].

- An end-to-end deep learning framework with multi-task loss function for simultaneous segmentation of leaf and diseased region using unified feature maps.
- To the best of our knowledge, this is the first study to quantify disease severity corresponding to individual leaves from UAV field images.

Although the results of the deep learning framework have been shown on maize plants, this end-to-end architecture can be easily generalized for localization and quantification of stress on other field plants. The rest of the paper is organized as follows: Section 2 describes the data annotations steps and in section 3, the proposed methodology is elucidated. Experimental results and analysis are given in Section 4 and section 5 concludes the paper.

2. Dataset

The UAV images of NLB infected maize plants [39] are used to show the effectiveness of our proposed framework for disease quantification. The first step of the phenotyping pipeline is the extraction of leaf instances. The leaf instance masks for these images were generated in a semi-automated fashion- Phenotiki [24]. This automated tool yields acceptable instances with input image and its corresponding segmented image. Thus, for precise leaf-level annotations, foreground segmentation (i.e. region of interest are plant leaves) of the field images was performed. In plant phenotyping literature, the majority of the algorithms assume strict conditions in terms of background content and utilise simplified heuristics for plant segmentation [22]. However, as previously mentioned, field images have complex backgrounds (soil), uneven illumination and perspective variability; thus these approaches fail for field images. Various texture-based algorithms [3, 22, 23] results in missed foreground regions with uneven illuminations. In addition, the color similarity between the diseased regions and soil results in the over-segmentation of the leaves in these regions. Thus, for a robust and accurate plant leaves segmentation, a statistical method, Mean-shift Bandwidths Searching Latent Dirichlet Allocation (MSBS-LDA) [37] was employed. Figure 1 shows the qualitative comparison of different segmentation algorithm, K-means [4] segmentation algorithm was also used, due to its widespread adoption in intensity-based plant segmentation.

Precise disease localization is essential to extract the phenotypic traits that quantify the disease’s severity for each leaf instance. However, the dataset and its corresponding labels generated by the authors in [39] are in the form of line markers corresponding to the main axis of the disease spots, not directly applicable for the disease quantification pipeline. Thus, the diseased regions were manually labeled with the help of VGG Image Annotator (VIA) [10], guided with the aforementioned line annotations [9].

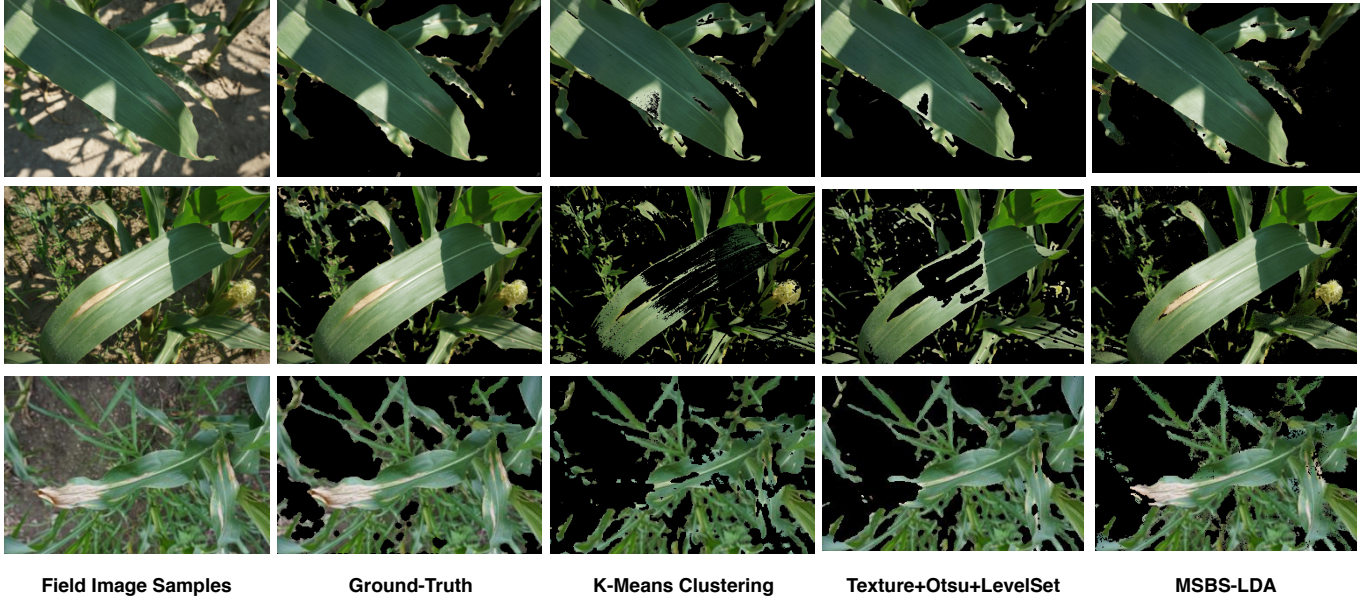


Figure 1. Qualitative comparison of different segmentation algorithms on field image data.

3. Methodology

The proposed deep learning architecture also termed as Cascaded MRCNN (shown in Figure 2) consists of a two-level approach for segmenting instances (leaves in our case) and the corresponding part segmentation (lesion spots for each leaf instance) in an end-to-end manner. We describe the design of the proposed framework in detail in the following subsection.

3.1. Cascaded MRCNN

Given the UAV field images and the corresponding annotated images containing leaf instances and diseased region, one approach to extract the phenotypic traits based on the segmented diseased region corresponding to an individual leaf is to (i) firstly segmenting the leaf instances using state-of-the-art architecture Mask R-CNN [16] followed by (ii) segmenting the diseased region for each leaf instance using Fully Convolutional Networks (FCN) [20], that is trained on the instances obtained from Mask R-CNN. However, this results in an additional overhead of training two networks and repetitive feature extraction. To overcome the aforementioned limitations, Cascaded MRCNN is designed that efficiently utilize the feature maps obtained during the leaf instance segmentation task. An additional mask branch (Cascaded Mask Branch) is introduced along with the Primary Mask Branch of Mask R-CNN architecture that learns to semantically segment the object sub-parts (diseased regions corresponding to leaves) from the encoded feature maps of the object regions (leaves). In contrast to cascading the feature maps presented in PSDet [41], the

feature maps is re-utilised to generate both the object and sub-object masks.

Training: To train our Cascaded MRCNN in an end-to-end fashion, a multi-task loss ($L_{Cascade}$) is used, defined as:

$$L_{Cascade} = L_{cls} + L_{box} + L_{primary-branch} + L_{cascaded-branch} \quad (1)$$

The classification loss L_{cls} , bounding box loss L_{box} and primary mask branch loss $L_{primary-branch}$ are identical as those defined in [16]. For each RoI, the cascaded mask branch outputs a $m \times m$ mask (\hat{M}) on which per pixel sigmoid is applied. A weighted pixel-wise cross entropy loss $L_{cascaded-branch}$ is used, defined as:

$$L_{cascaded-branch} = \sum_{y \in M, \hat{y} \in \hat{M}} [w_1 y \log(\hat{y}) + w_0 (1 - y) \log(1 - \hat{y})] \quad (2)$$

where M and \hat{M} are the ground truth and predicted sub-object masks. w_0 and w_1 are the class weights introduced because of the intra-class data imbalance. The values of w_0 and w_1 depends on the sub-object size. In our case, as the diseases region (class-1) on an average spans a small part of the leaf (empirically observed), thus we set $w_0 = 0.15$ and $w_1 = 0.85$. We trained our Cascaded MRCNN in an end-to-end manner on NLB infected field images of maize data (172 samples, 80:10:10 split, annotation details given in Section 2). To further increase the variability of the data,

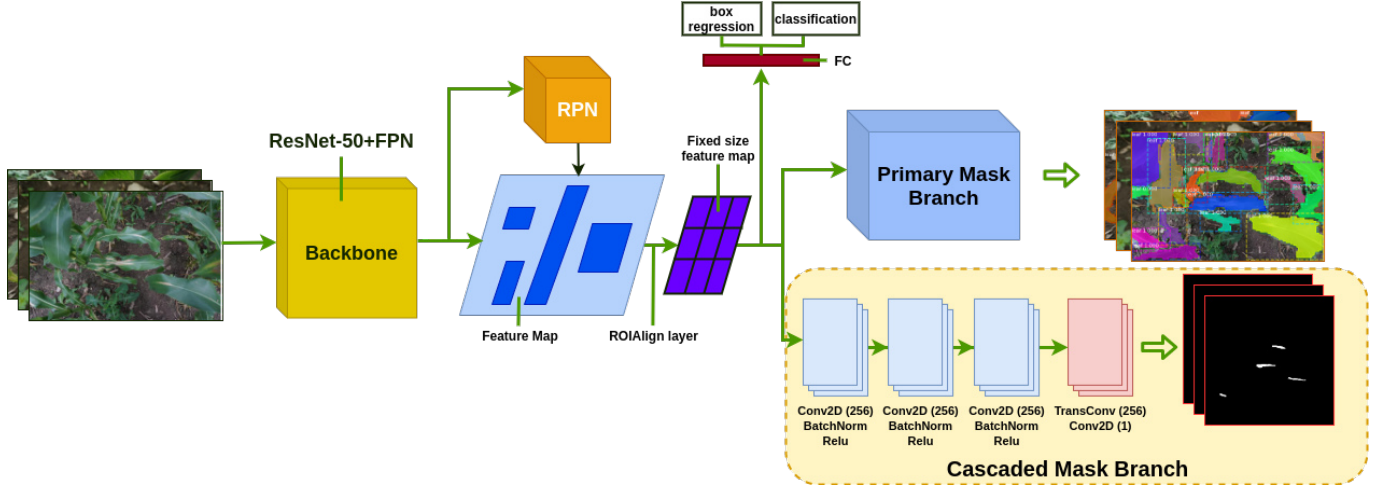


Figure 2. Cascaded MRCNN framework. Given an input image (i) Primary mask branch predicts individual leaf segments (Leaf instance segmentation) and a (ii) Cascaded mask branch is added that utilises the feature maps corresponding to leaf instances for generating diseased region mask

various geometric and color based augmentations were also applied.

An NVIDIA Quadro P5000 with 16 GB GDDR5 memory and 2560 Cuda cores was utilized for training.

4. Experimental Results

In this section, we show the effectiveness of the proposed framework evaluated using the following measures [29]:

Dice Accuracy: Dice Accuracy score is used to measure the degree of overlap between the predicted result (P^{pr}) and ground truth (P^{gt}) binary segmentation masks.

$$DiceAccuracy(\%) = \frac{2|P^{pr} \cap P^{gt}|}{|P^{pr}| + |P^{gt}|} \quad (3)$$

Symmetric Best Dice (SBD): To estimate the average leaf instance segmentation accuracy symmetric best dice is used. For each leaf instance the ground truth label yielding the maximum dice accuracy score is used and averaged over all the leaves.

$$BD(L^{pr}, L^{gt}) = \frac{1}{M} \sum_{i=1}^M \max_{1 \leq j \leq N} \frac{2|L_i^{pr} \cap L_j^{gt}|}{|L_i^{pr}| + |L_j^{gt}|} \quad (4)$$

$$SBD(L^{pr}, L^{gt}) = \min\{BD(L^{pr}, L^{gt}), BD(L^{gt}, L^{pr})\} \quad (5)$$

where L^{pr} and L^{gt} are predicted and ground truth leaf instance labels and $|\cdot|$ represents the area or the pixel count.

Difference in Count (DiC): To evaluate the precision of the algorithm in determining the correct number of leaves DiC is used.

$$DiC = \#L^{pr} - \#L^{gt} \quad (6)$$

Latency: To evaluate the runtime efficiency of the pipeline, latency (Inference time taken by 1 sample image) is evaluated. For deep learning models, reported Latency values are calculated using the NVIDIA Quadro P5000 GPU machine.

4.1. Baseline Method

Firstly, a disease phenotyping pipeline consisting of two steps: (1) leaf instance segmentation and (2) disease region segmentation is designed, where the deep neural networks corresponding to the two tasks (details given in the following subsections) are trained independently. We show the improved disease severity quantification performance in comparison with this baseline approach.

4.1.1 Leaf Instance Segmentation

In plant phenotyping literature, current methods for leaf instance segmentation primarily rely on either (i) extracting information from Euclidean distance map (EDM) of the segmented plant image or (ii) extracting leaf instances based on shape matching [29]. In addition, methods based on active shape models or deformable templates have been also proposed [21, 34]. However, these solutions were proposed for plant images captured in a controlled environment and for specific leaf shape characteristics, thus these methods fail in dense overlapping scenarios. To deal with

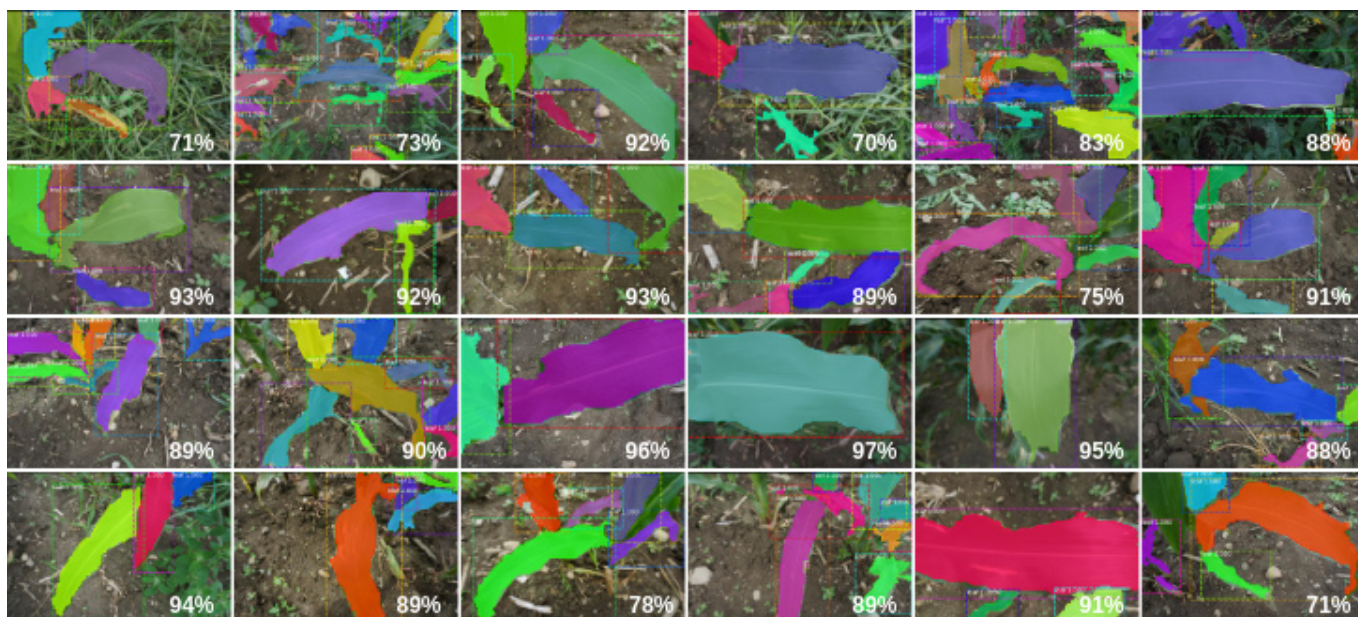


Figure 3. Leaf instance segmentation results of the proposed Cascaded MRCNN

occlusion, various deep neural networks based on recurrent neural network [28] and Mask R-CNN [16] have been proposed. Mask R-CNN achieved a Symmetric Best Dice (SBD) similarity score of 73% with the ground truth test data. The Non-Maximum Suppression (NMS) threshold is kept relatively high because of high degree of overlapped leaves. In contrast to Mask R-CNN, instance segmentation with recurrent attention performs sequential analysis of the input image to deal with complex object distributions and make predictions that are coherent with each other. A SBD similarity score of 76% on the same test data was obtained using this network. The symmetric best dice (SBD), difference in count (DiC) and the latency values along with corresponding standard deviations are reported for each method in Table 1 and a qualitative comparison is shown in Figure 4.

4.1.2 Diseased Region Segmentation

Within the phenotyping literature, segmentation algorithm proposed for disease region segmentation [19] were utilised for comparison with the proposed framework. Conventional machine learning algorithms like K-means [15] and Gaussian mixture model (GMM) [26] with color and texture features generated noisy images, as shown in Figure 5; this is due to the similarity of the diseased region with the background (soil). Also, in some of the images with uneven illuminations and mosses, these algorithms fail to give the desired results. Compared to the deep learning models, these previously discussed approaches have low representation ability, consequently we also compared the proposed

framework with Fully Convolutional Networks (FCN) [20] & SegNet [6]. These networks trained with our annotated data augmented with various noises were able to segment the diseased region with a dice accuracy of 92%.

Methods (leaf instance)	SBD	DiC	Latency
Marker Controlled Watershed	0.61 ± .08	3.4 ± 1.7	1.9 ± .38
Mask-RCNN	0.73 ± .10	1.6 ± 1.2	0.2 ± .05
Recurrent Attention	0.76 ± .09	0.9 ± .51	0.5 ± .14
Cascaded MRCNN	0.74 ± .12	1.1 ± .7	0.2 ± .09

Table 1. Symmetric Best Dice, Difference in Count and Latency values of the different methods and the Primary Mask Branch of the proposed Cascaded MRCNN.

Methods (Diseased Region)	Dice Accuracy	Latency
K-means	0.49 ± .08	0.94 ± .32
Texture + Otsu	0.51 ± .07	0.07 ± .028
GMM	0.64 ± .05	1.08 ± .46
SegNet	0.91 ± .04	0.06 ± .03
FCN	0.92 ± .03	0.08 ± .02
Cascaded MRCNN	0.91 ± .06	0.2 ± .09

Table 2. Dice Accuracy and Latency of different baseline methods and Cascaded Mask Branch of the proposed Cascaded MRCNN for disease region segmentation.

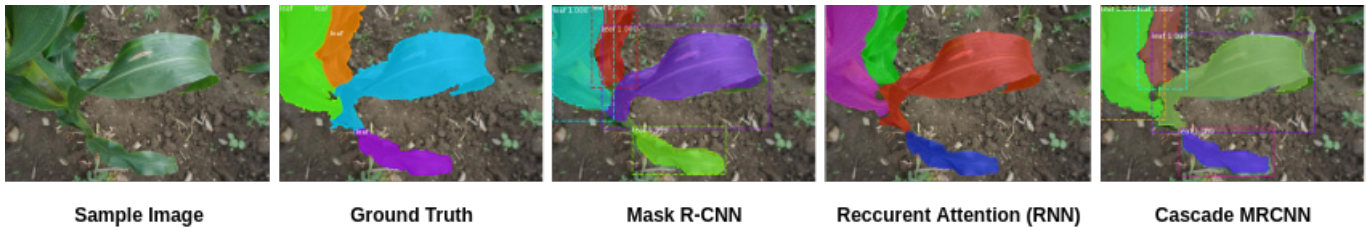


Figure 4. Example instance segmentation results of different methods

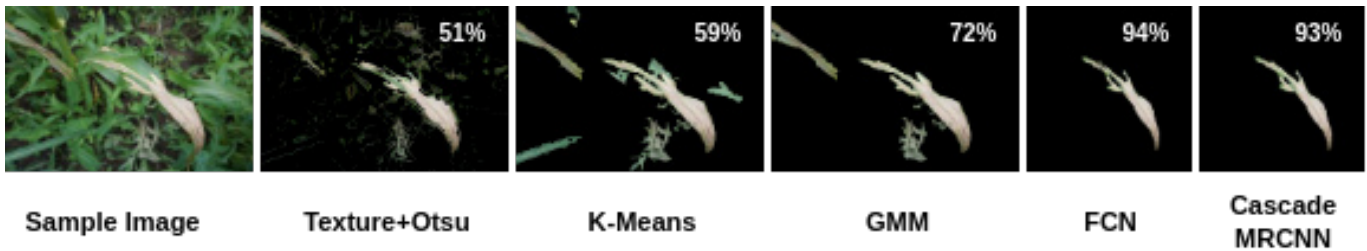


Figure 5. Selected result with different segmentation algorithms to extract the diseased region (Top right shows the Dice Accuracy scores)

4.2. Cascaded MRCNN

To reduce the overhead of training two networks for this task and to efficiently reuse the features extracted from the image, we designed an end to end pipeline Cascaded MR-CNN. The proposed framework follows a single stream approach i.e extracting the disease regions from the feature maps of each leaf instance. Cascaded MRCNN successfully segments the leaf and diseased regions from the image with a Dice accuracy of 91% for disease region segmentation and an SBD similarity score of 74% for leaf instance segmentation.

4.3. Disease Quantification

Disease severity has been defined as the ratio of the area of the diseased region to the area of the infected leaf [30], given as follows:

$$\text{Severity Index (SI)} = \frac{\text{Diseased region area}}{\text{Leaf area}} \quad (7)$$

In this paper, an ablation study with respect to the state-of-the-art algorithms for leaf instance and diseased region segmentation was conducted to design an efficient architecture for severity quantification. The correlation and the mean square error (MSE) between the predicted and ground truth SI were used as evaluation metrics. Experimental analysis and comparisons with different model selection in the parallel pipeline show that the recurrent attention module (for Leaf Instance Segmentation) with the FCN (for diseased region segmentation) achieves a correlation of 71% and MSE of 3.0094. Whereas the SI computed with the

Severity Quantification (Correlation)

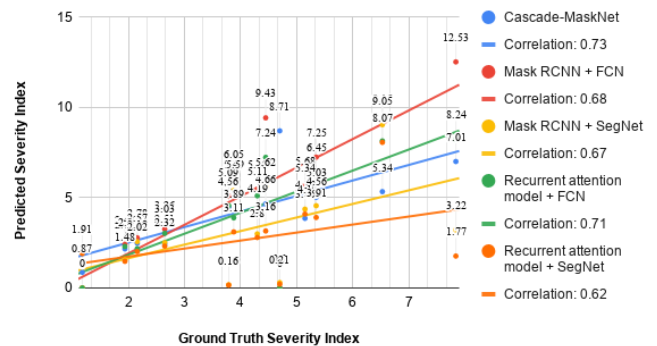


Figure 6. Correlation plot of predicted SI with ground truth SI

proposed framework shows a 73% correlation and MSE (2.0437). Figure 6 shows the correlation plot and Table 3 summarizes the correlation and MSE metrics.

5. Conclusion

In this paper, we introduced a deep learning framework (Cascaded MRCNN), for disease quantification based on field images. In contrast to the current disease phenotyping methods, that classify the presence or absence of diseases in the field images, our proposed framework yield disease severity based on segmentation of diseased region corresponding to each leaf instance in an end-to-end manner, that permits high-throughput and non-invasive screening of fields, crucial for the selection of disease-resistant crops.

Leaf Instance Segmentation	Diseased Region Segmentation	Design	MSE	Correlation
Mask R-CNN	FCN	Parallel	4.4423	0.68
Mask R-CNN	SegNet	Parallel	4.3053	0.67
Recurrent attention model	FCN	Parallel	3.0094	0.71
Recurrent attention model	SegNet	Parallel	4.0219	0.62
Cascaded MRCNN	–	End to End	2.0437	0.73

Table 3. Correlation and MSE based on predicted SI and ground truth SI

Acknowledgement. This work is supported by National Agricultural Science Fund (NASF) under Indian Council of Agricultural Research (ICAR), Delhi, India [Artificial Intelligence Based Mobile App for Identification and advisory of Maize Diseases and Insect Pests].

References

- [1] Heba Al-Hiary, Sulieman Bani-Ahmad, M Reyalat, Malik Braik, and Zainab Alrahamneh. Fast and accurate detection and classification of plant diseases. *International Journal of Computer Applications*, 17(1):31–38, 2011.
- [2] Jihen Amara, Bassem Bouaziz, and Alsayed Algergawy. A deep learning-based approach for banana leaf diseases classification. *Datenbanksysteme für Business, Technologie und Web (BTW 2017)-Workshopband*, 2017.
- [3] Sai Arivazhagan, R Newlin Shebiah, S Ananthi, and S Vishnu Varthini. Detection of unhealthy region of plant leaves and classification of plant leaf diseases using texture features. *Agricultural Engineering International: CIGR Journal*, 15(1):211–217, 2013.
- [4] David Arthur and Sergei Vassilvitskii. k-means++: The advantages of careful seeding. Technical report, Stanford, 2006.
- [5] Yousef Atoum, Muhammad Jamal Afridi, Xiaoming Liu, J Mitchell McGrath, and Linda E Hanson. On developing and enhancing plant-level disease rating systems in real fields. *Pattern Recognition*, 53:287–299, 2016.
- [6] Vijay Badrinarayanan, Alex Kendall, and Roberto Cipolla. Segnet: A deep convolutional encoder-decoder architecture for image segmentation. *IEEE transactions on pattern analysis and machine intelligence*, 39(12):2481–2495, 2017.
- [7] A Camargo and JS Smith. An image-processing based algorithm to automatically identify plant disease visual symptoms. *Biosystems engineering*, 102(1):9–21, 2009.
- [8] Joaquin J Casanova, Susan A O’Shaughnessy, Steven R Evett, and Charles M Rush. Development of a wireless computer vision instrument to detect biotic stress in wheat. *Sensors*, 14(9):17753–17769, 2014.
- [9] Chad DeChant, Tyr Wiesner-Hanks, Siyuan Chen, Ethan L Stewart, Jason Yosinski, Michael A Gore, Rebecca J Nelson, and Hod Lipson. Automated identification of northern leaf blight-infected maize plants from field imagery using deep learning. *Phytopathology*, 107(11):1426–1432, 2017.
- [10] Abhishek Dutta, Ankush Gupta, and Andrew Zissermann. Vgg image annotator (via). URL: <http://www.robots.ox.ac.uk/~vgg/software/via>, 2016.
- [11] Konstantinos P Ferentinos. Deep learning models for plant disease detection and diagnosis. *Computers and Electronics in Agriculture*, 145:311–318, 2018.
- [12] Fabio Fiorani and Ulrich Schurr. Future scenarios for plant phenotyping. *Annual review of plant biology*, 64:267–291, 2013.
- [13] Robert T Furbank and Mark Tester. Phenomics—technologies to relieve the phenotyping bottleneck. *Trends in plant science*, 16(12):635–644, 2011.
- [14] Esmael Hamuda, Martin Glavin, and Edward Jones. A survey of image processing techniques for plant extraction and segmentation in the field. *Computers and Electronics in Agriculture*, 125:184–199, 2016.
- [15] John A Hartigan and Manchek A Wong. Algorithm as 136: A k-means clustering algorithm. *Journal of the royal statistical society. series c (applied statistics)*, 28(1):100–108, 1979.
- [16] Kaiming He, Georgia Gkioxari, Piotr Dollár, and Ross Girshick. Mask r-cnn. In *Proceedings of the IEEE international conference on computer vision*, pages 2961–2969, 2017.
- [17] Kuo-Yi Huang. Application of artificial neural network for detecting phalaenopsis seedling diseases using color and texture features. *Computers and Electronics in agriculture*, 57(1):3–11, 2007.
- [18] Yann LeCun, Yoshua Bengio, and Geoffrey Hinton. Deep learning. *nature*, 521(7553):436–444, 2015.
- [19] Ke Lin, Liang Gong, Yixiang Huang, Chengliang Liu, and Junsong Pan. Deep learning-based segmentation and quantification of cucumber powdery mildew using convolutional neural network. *Frontiers in plant science*, 10:155, 2019.
- [20] Jonathan Long, Evan Shelhamer, and Trevor Darrell. Fully convolutional networks for semantic segmentation. In *Proceedings of the IEEE conference on computer vision and pattern recognition*, pages 3431–3440, 2015.
- [21] A-G Manh, G Rabatel, Louis Assemat, and M-J Aldon. Ae—automation and emerging technologies: weed leaf image segmentation by deformable templates. *Journal of agricultural engineering research*, 80(2):139–146, 2001.
- [22] Massimo Minervini, Mohammed M Abdelsamea, and Sotirios A Tsafaris. Image-based plant phenotyping with incremental learning and active contours. *Ecological Informatics*, 23:35–48, 2014.

- [23] Massimo Minervini, Mohammed M Abdelsamea, and Sotirios A Tsafaris. Image-based plant phenotyping with incremental learning and active contours. *Ecological Informatics*, 23:35–48, 2014.
- [24] Massimo Minervini, Mario V Giuffrida, Pierdomenico Perata, and Sotirios A Tsafaris. Phenotiki: An open software and hardware platform for affordable and easy image-based phenotyping of rosette-shaped plants. *The Plant Journal*, 90(1):204–216, 2017.
- [25] Sharada P Mohanty, David P Hughes, and Marcel Salathé. Using deep learning for image-based plant disease detection. *Frontiers in plant science*, 7:1419, 2016.
- [26] Thanh Minh Nguyen and QM Jonathan Wu. Fast and robust spatially constrained gaussian mixture model for image segmentation. *IEEE transactions on circuits and systems for video technology*, 23(4):621–635, 2012.
- [27] Santanu Phadikar, Jaya Sil, and Asit Kumar Das. Classification of rice leaf diseases based on morphological changes. *International Journal of Information and Electronics Engineering*, 2(3):460–463, 2012.
- [28] Amaia Salvador, Miriam Bellver, Victor Campos, Manel Baradad, Ferran Marques, Jordi Torres, and Xavier Giro-i Nieto. Recurrent neural networks for semantic instance segmentation. *arXiv preprint arXiv:1712.00617*, 2017.
- [29] Hanno Scharr, Massimo Minervini, Andrew P French, Christian Klukas, David M Kramer, Xiaoming Liu, Imanol Luengo, Jean-Michel Pape, Gerrit Polder, Danijela Vukadinovic, et al. Leaf segmentation in plant phenotyping: a collation study. *Machine vision and applications*, 27(4):585–606, 2016.
- [30] Malusi Sibiyi and Mbuyu Sumbwanyambe. An algorithm for severity estimation of plant leaf diseases by the use of colour threshold image segmentation and fuzzy logic inference: a proposed algorithm to update a “leaf doctor” application. *AgriEngineering*, 1(2):205–219, 2019.
- [31] Arti Singh, Baskar Ganapathysubramanian, Asheesh Kumar Singh, and Soumik Sarkar. Machine learning for high-throughput stress phenotyping in plants. *Trends in plant science*, 21(2):110–124, 2016.
- [32] Asheesh Kumar Singh, Baskar Ganapathysubramanian, Soumik Sarkar, and Arti Singh. Deep learning for plant stress phenotyping: trends and future perspectives. *Trends in plant science*, 23(10):883–898, 2018.
- [33] Srdjan Sladojevic, Marko Arsenovic, Andras Anderla, Dubravko Culibrk, and Darko Stefanovic. Deep neural networks based recognition of plant diseases by leaf image classification. *Computational intelligence and neuroscience*, 2016, 2016.
- [34] Henning Tangen Sjøgaard. Weed classification by active shape models. *Biosystems engineering*, 91(3):271–281, 2005.
- [35] Ethan L Stewart, Tyr Wiesner-Hanks, Nicholas Kaczmar, Chad DeChant, Harvey Wu, Hod Lipson, Rebecca J Nelson, and Michael A Gore. Quantitative phenotyping of northern leaf blight in uav images using deep learning. *Remote Sensing*, 11(19):2209, 2019.
- [36] Guan Wang, Yu Sun, and Jianxin Wang. Automatic image-based plant disease severity estimation using deep learning. *Computational intelligence and neuroscience*, 2017, 2017.
- [37] Yi Wang and Lihong Xu. Unsupervised segmentation of greenhouse plant images based on modified latent dirichlet allocation. *PeerJ*, 6:e5036, 2018.
- [38] Shen Weizheng, Wu Yachun, Chen Zhanliang, and Wei Hongda. Grading method of leaf spot disease based on image processing. In *2008 international conference on computer science and software engineering*, volume 6, pages 491–494. IEEE, 2008.
- [39] Tyr Wiesner-Hanks, Ethan L Stewart, Nicholas Kaczmar, Chad DeChant, Harvey Wu, Rebecca J Nelson, Hod Lipson, and Michael A Gore. Image set for deep learning: field images of maize annotated with disease symptoms. *BMC research notes*, 11(1):440, 2018.
- [40] Patrick Wspanialy and Medhat Moussa. Early powdery mildew detection system for application in greenhouse automation. *Computers and Electronics in Agriculture*, 127:487–494, 2016.
- [41] Zizhang Wu, Weiwei Sun, Man Wang, Xiaoquan Wang, Lizhu Ding, and Fan Wang. Psdet: Efficient and universal parking slot detection. *arXiv preprint arXiv:2005.05528*, 2020.
- [42] Zhong-Qiu Zhao, Peng Zheng, Shou-tao Xu, and Xindong Wu. Object detection with deep learning: A review. *IEEE transactions on neural networks and learning systems*, 30(11):3212–3232, 2019.